

REPORT

Long-range signaling by phosphoprotein waves arising from bistability in protein kinase cascades

Nick I Markevich¹, Mikhail A Tsyganov¹, Jan B Hoek and Boris N Kholodenko*

Department of Pathology, Anatomy and Cell Biology, Thomas Jefferson University, Locust St, Philadelphia, PA, USA

* Corresponding author. Department of Pathology, Anatomy and Cell Biology, Thomas Jefferson University, 1020 Locust St, Philadelphia, PA 19107, USA.

Tel.: +1 215 503 1614; Fax: +1 215 923 2218; E-mail: boris.kholodenko@jefferson.edu

¹ These authors contributed equally to this work

Received 10.7.06; accepted 2.10.06

A hallmark of protein kinase/phosphatase cascades, including mitogen-activated protein kinase (MAPK) pathways, is the spatial separation of their components within cells. The top-level kinase, MAP3K, is phosphorylated at the cell membrane, and cytoplasmic kinases at sequential downstream levels (MAP2K and MAPK) spread the signal to distant targets. Given measured protein diffusivity and phosphatase activities, signal propagation by diffusion would result in a steep decline of MAP2K activity and low bisphosphorylated MAPK (ppMAPK) levels near the nucleus, especially in large cells, such as oocytes. Here, we show that bistability in a two-site MAPK (de)phosphorylation cycle generates a novel type of phosphoprotein wave that propagates from the surface deep into the cell interior. Positive feedback from ppMAPK to cytoplasmic MAP2K enhances the propagation span of the ppMAPK wave, making it possible to convey phosphorylation signals over exceedingly long distances. The finding of phosphorylation waves traveling with constant amplitude and high velocity may solve a long-standing enigma of survival signaling in developing neurons.

Molecular Systems Biology 14 November 2006; doi:10.1038/msb4100108

Subject Categories: simulation and data analysis; signal transduction

Keywords: bistable switches; long-range signaling; MAPK cascades; phosphorylation waves; retrograde signaling in developing neurons

Introduction

Cascades of coupled phosphorylation/dephosphorylation cycles, such as mitogen-activated protein kinase (MAPK) pathways, integrate external stimuli and propagate signals from the plasma membrane (PM) to the nucleus. A typical, three-tier cascade comprises MAPK, MAPK kinase (MAP2K) and MAP2K kinase (MAP3K). MAP2K is activated by MAP3K at the cell membrane and then drifts into the cell interior, where it phosphorylates MAPK on two conserved threonine and tyrosine residues. Various phosphatases reverse these phosphorylations. The biological outcome of stimulation depends on the temporal profile of active, bisphosphorylated MAPK (ppMAPK) in the perinuclear area (Murphy *et al*, 2002).

Owing to dephosphorylation during diffusion through the cytoplasm, the phosphorylation level of downstream kinases may become low near the nucleus. In fact, for a protein phosphorylated by a membrane-bound kinase and dephosphorylated by a cytosolic phosphatase, Brown and Kholodenko (1999) showed that there can be a precipitous spatial gradient of the phosphorylated form, high close to the membrane and low within the cell. The existence of a phosphoprotein gradient of this kind has been confirmed

theoretically (Lipkow *et al*, 2005) and experimentally (Kalab *et al*, 2002; Niethammer *et al*, 2004). Additional tiers in a kinase cascade can make shallower the phosphoprotein gradients (Kholodenko, 2006); yet signaling across a distance of more than about 5–10 μm requires more than diffusion. This includes (i) trafficking of phosphorylated kinases within endocytic vesicles or non-vesicular signaling complexes by molecular motors (Kholodenko, 2002; Howe and Mobley, 2004; Miaczynska *et al*, 2004; Perlson *et al*, 2005) and (ii) phosphoprotein waves propagating from the membrane over long distances, especially in large cells, such as *Xenopus* oocytes (Kholodenko, 2003; Slepchenko and Terasaki, 2003). Phosphoprotein waves may also be a key to the long-standing enigma of retrograde signaling in developmental neurons, where tyrosine phosphorylation in neuron bodies starts as early as a few minutes after nerve growth factor (NGF) stimulation of distal axons located centimeters away (MacInnis *et al*, 2003). Such a rapid propagation of survival signals over centimeters of axon length cannot be accounted for by the retrograde transport of endosomes or translocation of phosphorylated kinases by molecular motors moving with rates of a few $\mu\text{m/s}$ (Hill *et al*, 2004). An alternative mechanism for the initial, rapid transfer of phosphorylation signals might be

phosphoprotein waves that travel from the distal axon to the neuron body (Kholodenko, 2003).

A phosphoprotein wave amplifies the phosphorylation level at the wave front following the arrival of active molecules by diffusion. This local amplification can arise from a positive feedback enabling reaction cascades to display switch-like, bistable behavior. In fact, traveling waves in bistable systems are known in physics, chemistry and biology (Zhabotinsky and Zaikin, 1973; Keener and Sneyd, 1998; Reynolds *et al*, 2003). For MAPK cascades, bistability is thought to arise from activation of kinases at the top of the cascade (MAP3K) by downstream kinase (MAPK) (Bhalla *et al*, 2002; Xiong and Ferrell, 2003). However, these long positive feedback loops will increase the phosphorylation levels close to the PM where activated MAP3K is localized, but not at distant cytoplasmic areas. To bring about phosphoprotein waves, kinases in the cytoplasm should exhibit bistability, as the intrinsically bistable MAPK cycle does (Markevich *et al*, 2004). Importantly, a theoretical prediction that a two-site MAPK phosphorylation circuit can generate bistability was recently confirmed experimentally for the extracellular signal-regulated kinase (ERK) cycle in BHK cells (Harding *et al*, 2005) and for the Fus3/MAPK cycle in yeast (Wang *et al*, 2006).

In the present paper, we demonstrate a novel type of phosphoprotein wave that emerges from the bistable behavior of kinase and phosphatase circuits in the cytoplasm and relays extracellular signals from the PM to distant targets. We unveil how the transfer of phosphorylation signals depends on the input–output relationships of sequential cascade levels. The findings show that bistability intrinsic to the MAPK activation cycle can give rise to a wave of active MAPK that propagates a binary phosphorylation signal. Positive feedback from MAPK to cytoplasmic MAP2K enables this wave to propagate with high velocity over exceedingly long distances. These traveling waves of protein phosphorylation present a novel mechanism of long-range signaling within cells, when phosphorylation signals cannot be transferred by diffusion. We demonstrate how waves of phosphorylated kinases may be involved in retrograde signaling in neurons.

Results and discussion

Computational analysis of the spatio-temporal dynamics

Our MAPK cascade models explicitly incorporate heterogeneous spatial distribution of activated kinases. For illustrative

Table I Equations and boundary conditions describing the dynamics of MAP cascade kinases

	Equations	Boundary conditions
1	$d[\text{pMAP3K}]/dt = v_1^m - v_2^m$	
2	$\frac{\partial[\text{pMAP2K}]}{\partial t} = \left(\frac{D}{L^2}\right) \times \frac{1}{x^2} \frac{\partial}{\partial x} \left(x^2 \frac{\partial[\text{pMAP2K}]}{\partial x} \right) + v_5^c - v_6^c$	$\frac{\partial[\text{pMAP2K}]}{\partial x} \Big _{x=1} = \frac{L^2}{3D} (v_3^m - v_4^m + v_5^m - v_6^m)$ $\frac{\partial[\text{pMAP2K}]}{\partial x} \Big _{x=Q/L} = 0$
3	$\frac{\partial[\text{ppMAP2K}]}{\partial t} = \left(\frac{D}{L^2}\right) \frac{1}{x^2} \frac{\partial}{\partial x} \left(x^2 \frac{\partial[\text{ppMAP2K}]}{\partial x} \right) - v_5^c$	$\frac{\partial[\text{ppMAP2K}]}{\partial x} \Big _{x=1} = \frac{L^2}{3D} (v_4^m - v_5^m)$ $\frac{\partial[\text{ppMAP2K}]}{\partial x} \Big _{x=Q/L} = 0$
4	$\frac{\partial[\text{pMAPK}]}{\partial t} = \left(\frac{D}{L^2}\right) \frac{1}{x^2} \frac{\partial}{\partial x} \left(x^2 \frac{\partial[\text{pMAPK}]}{\partial x} \right) + v_7^c - v_8^c + v_9^c - v_{10}^c$	$\frac{\partial[\text{pMAPK}]}{\partial x} \Big _{x=1} = 0$ $\frac{\partial[\text{pMAPK}]}{\partial x} \Big _{x=Q/L} = 0$
5	$\frac{\partial[\text{ppMAPK}]}{\partial t} = \left(\frac{D}{L^2}\right) \frac{1}{x^2} \frac{\partial}{\partial x} \left(x^2 \frac{\partial[\text{ppMAPK}]}{\partial x} \right) + v_8^c - v_9^c$	$\frac{\partial[\text{ppMAPK}]}{\partial x} \Big _{x=1} = 0$ $\frac{\partial[\text{ppMAPK}]}{\partial x} \Big _{x=Q/L} = 0$

L is the cell radius, Q is the nuclear radius, D is the diffusivity of proteins in the cytosol (for illustrative purposes, assumed to be equal to $2 \mu\text{m}^2/\text{s}$ for both the phosphorylated and unphosphorylated forms) and x is a dimensionless coordinate, equal to the distance from the cell center divided by the cell radius, L . The distance d from the cell membrane is expressed in terms of x as, $d = (1-x)L$. The rate expressions are given in Tables II and III.

purposes, we initially consider a spherical cell of radius $L=15\ \mu\text{m}$ with a nucleus of radius $Q=6\ \mu\text{m}$ (Supplementary Figure S1). Much larger distances up to centimeters and one-dimensional geometry are considered for long-range signaling in developing neurons. The spatio-temporal dynamics of the MAPK cascade is described by partial differential equations (known as reaction–diffusion equations; Table I).

Cell size (L) and protein diffusivity (D) influence the spatio-temporal dynamics as a single parameter combination L^2/D , known as the ‘diffusion-time’ (Table I). The protein diffusivity in the cytoplasm was reported to be in a range of $1\text{--}10\ \mu\text{m}^2/\text{s}$ (reviewed by Brown and Kholodenko, 1999). For illustrative purposes, we assume $D=2\ \mu\text{m}^2/\text{s}$ under ‘crowded’ cytoplasmic condition (Khan *et al*, 2004). The assumption of higher limit of D -values of $10\ \mu\text{m}^2/\text{s}$ will not change our findings, if traveling distances (L) increase approximately two-fold. Importantly, variations in the reported diffusivity values do

not change our conclusion of inability of diffusion to propagate phosphorylation signals over distances of tens of micrometers and our analysis of long-range signaling in neurons.

Stimulus–response relationships and the spatial propagation of the signals

How well MAPK phosphorylation spreads into the cell crucially depends on the feedback design and input–output relationships of sequential MAPK cascade levels. The basic feature of MAPK cascades is their intrinsic potential for the sensitivity amplification known as ultrasensitivity, a term coined by Goldbeter and Koshland 25 years ago. Steeply sigmoidal responses of ppMAPK to changes in the levels of ppMAP2K shown in Figure 1A and Ras-GTP/MAP3K (inset to Figure 1A) are brought about by the multiplication of the sensitivities and dual phosphorylation (Brown *et al*, 1997;

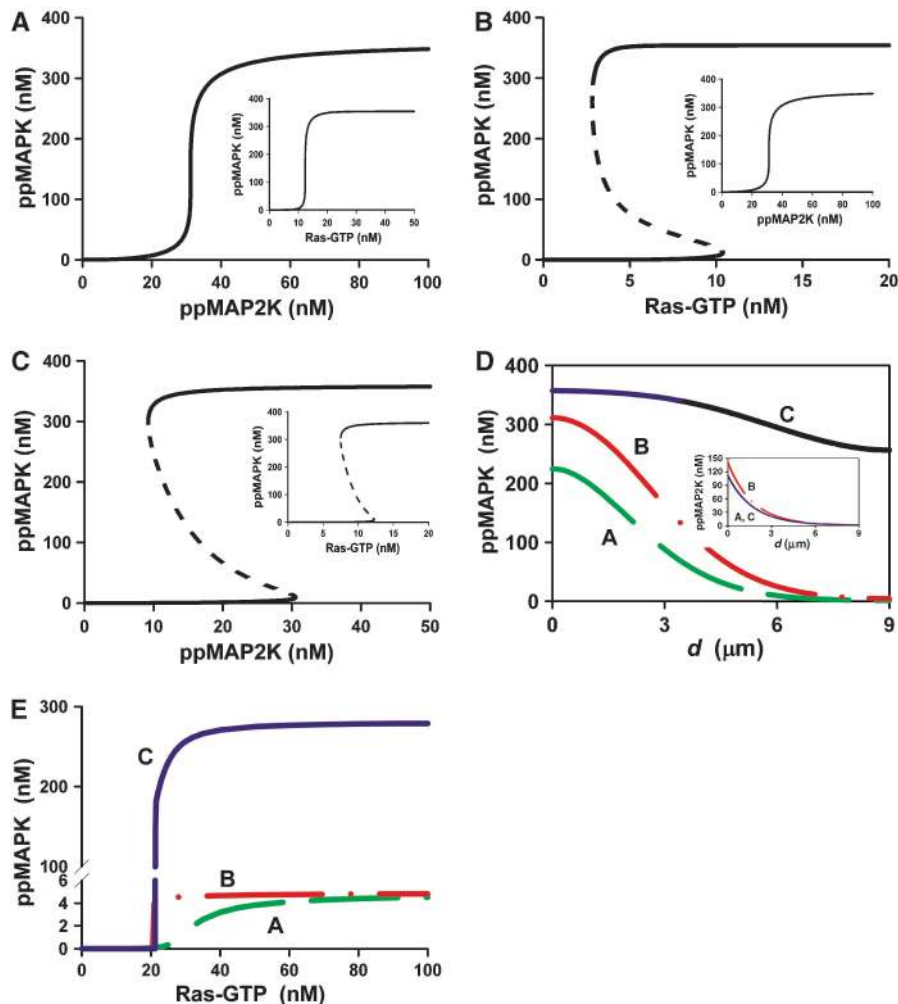


Figure 1 Spatial propagation of MAPK activation for the three different feedback designs and input–output relationships of MAPK cascades. **(A)** Ultrasensitive steady-state dependence of ppMAPK on the active MAP2K (ppMAP2K). The stationary dependence of ppMAPK on Ras-GTP is shown in the inset. **(B)** Hysteresis in the MAPK response to Ras stimulation brought about by a positive feedback from ppMAPK to Ras/MAP3K. The kinetic parameters of the MAPK cycle are the same as for panel A. The corresponding stationary dependence of ppMAPK on ppMAP2K is shown in the inset. **(C)** Bistable dependence of bisphosphorylated ERK (ppMAPK) on active MEK (ppMAP2K). **(D)** Stationary spatial profiles of ppMAPK and ppMAP2K (inset to panel D) across the cell diameter for three different stimulus–response dependencies shown in panels A–C. **(E)** The dependences of the stationary ppMAPK level at the nuclear membrane on the magnitude of sustained Ras signal at the PM. In panels D and C, dashed (green), dashed-dot (red) and solid (blue) lines correspond to three different feedback designs A–C. See Tables I–III for the differential equations and parameters.

Ferrell, 1997). A long positive feedback further increases the steepness of the input–output relationship, making it similar to a step-function and allowing MAPK cascades to operate as bistable switches (Bhalla *et al*, 2002). For an MAPK cascade imbedded in a long positive feedback, Figure 1B illustrates bistable responses of ppMAPK to external stimuli (Ras-GTP) and ultrasensitive responses to ppMAP2K (inset to Figure 1B). Importantly, the two-site phosphorylation and dephosphorylation MAPK cycle by itself can already exhibit bistability (Figure 1C). In this cycle, the same ppMAP2K level can switch MAPK into either an active or inactive state, depending on whether the initial MAPK concentration was higher or lower than the value corresponding to an unstable state (dashed line).

When MAP2K is phosphorylated at the cell surface and dephosphorylated while drifting in the cytoplasm, spatial gradients of ppMAP2K are generated both before and at steady state. A strong decline in ppMAP2K with the distance from the membrane causes the ppMAPK fraction to decrease, reaching a nadir in the perinuclear area. For the three stimulus–response relationships shown in Figure 1A–C (one ultrasensitive and two mechanistically distinct, bistable responses of MAPK), Figure 1D compares steady-state spatial profiles of ppMAPK (inset to Figure 1D shows ppMAP2K profiles) activated by a sustained elevation of Ras-GTP/MAP3K levels (snapshots of ppMAPK and ppMAP2K spatial profiles at different times following the onset of activation are shown in Supplementary Figure S2). When the response is ultrasensitive (line A) or if bistability arises from a long feedback (line B), MAPK activity in the perinuclear area appears to be surprisingly low. Only when hysteresis occurs in the cytoplasm (line C) are ppMAPK concentrations near the PM and the nucleus similar, despite a precipitous decline in ppMAP2K. In fact, although the MAPK-induced feedback stimulation of cell-surface MAP3K increases MAP2K activity close to the membrane, this feedback is unable to substantially increase ppMAPK concentration deep in the cytoplasm (inset to Figure 1D). As a result, for all three distinct kinetic scenarios of signaling from MAP3K to MAPK, the level of ppMAP2K in the perinuclear area is roughly the same. Bistability within the MAPK cycle allows for self-perpetuation of MAPK activation all the way down to the nucleus, where MAP2K activity is low.

We may ask whether a significant increase in sustained Ras/MAP3K activity enhances MAPK signaling in the perinuclear area. Figure 1E demonstrates that although for all three feasible mechanisms of MAPK responses shown in Figure 1A–C, the stationary ppMAPK level near the nucleus increases with the magnitude of the sustained Ras-GTP activity, the maximal ppMAPK signal appears to be spectacularly higher when its propagation is supported by hysteresis in the MAPK cycle (line C). Positive feedback from MAPK to membrane-confined MAP3K may slightly decrease the amount of Ras-GTP needed for half-maximal MAPK activation (line B), but has practically no effect on the maximal achievable perinuclear level of ppMAPK, which is similar to that obtained for a merely sigmoidal response (line A). We conclude that MAPK bistability in the cytoplasm aids in the relay of phosphorylation cues.

Activation of cell-surface receptors is usually transient and results in a transient rather than sustained activation of Ras/

MAP3K at the cell membrane. The analysis of a transient stimulation of the MAPK cascade confirms the results shown for a sustained activation: the peak ppMAPK level near the nucleus is similar to the level near the cell surface only when the relay of the phosphorylated signal is enhanced by bistability in the MAPK cycle in the cytoplasm (Supplementary Figure S3). Supplementary Figure S4 further confirms this conclusion and illustrates how MAPK activation spreads in the space and eventually vanishes following a transient stimulation of Ras at the PM. Importantly, calculations also suggest that even a marked decrease in the phosphorylated MAPK fraction seen in the perinuclear area may not be readily detectable when ppMAPK is averaged over the whole cell (Supplementary Figure S3B), as it occurs for usual Western blot protocols.

Regulation of phosphatase activities plays a crucial role in signal propagation

Minimal qualitative models of phosphorylation spreading suggest that at large distances from the membrane, the steady-state phosphorylation signal declines approximately as the reciprocal of the exponent of the dimensionless parameter α (Kholodenko, 2002). The parameter α is the ratio of the diffusion time (proportional to the cell size squared L^2 , divided by the diffusivity D) and the dephosphorylation time (the reciprocal of phosphatase activity) and is recognizable as the Damkohler number. Our mechanistic models also suggest that a large increase in the cell size (diameter over 50 μm) results in a strong decline in the ppMAPK levels near the nucleus, even when MAPK bistability supports phosphorylation waves (Supplementary Figure S5). A molecular mechanism to facilitate such waves may involve inhibition of the phosphatase of MAP2K by active MAPK or this inhibition may occur concurrently with MAPK activation due to the production of reactive oxygen species triggered by growth factor stimulation (Kim *et al*, 2003). Inhibition of the MAP2K phosphatase generates positive feedback that expands the bistability range for the MAPK cycle (Kholodenko, 2006), as illustrated in Supplementary Figure S6. Most importantly, any mechanism of inhibition together with bistable MAPK cycle makes it possible to propagate the ppMAPK wave over distances of the order of 100 μm . Figures 2 and Supplementary Figure S7 illustrate this for a cell with a radius of 50 μm , such as oocytes. The wave of ppMAPK propagates to the nucleus in a few minutes and retains the magnitude of the ppMAPK fraction.

Long-range signaling via protein kinase cascades

A critical challenge confronting neurobiology is to understand how neurons transfer signals over long distances. The survival of developing neurons depends on neurotrophins, such as NGF, and its receptor TrkA. NGF produced by peripheral tissues binds to TrkA on distal axons, located up to 1 m away from the neuronal soma. How does the survival signal propagate over this remarkably long distance in a physiologically relevant span of time? Diffusion is ruled out, as it would be prohibitively slow. The prevalent model is receptor-

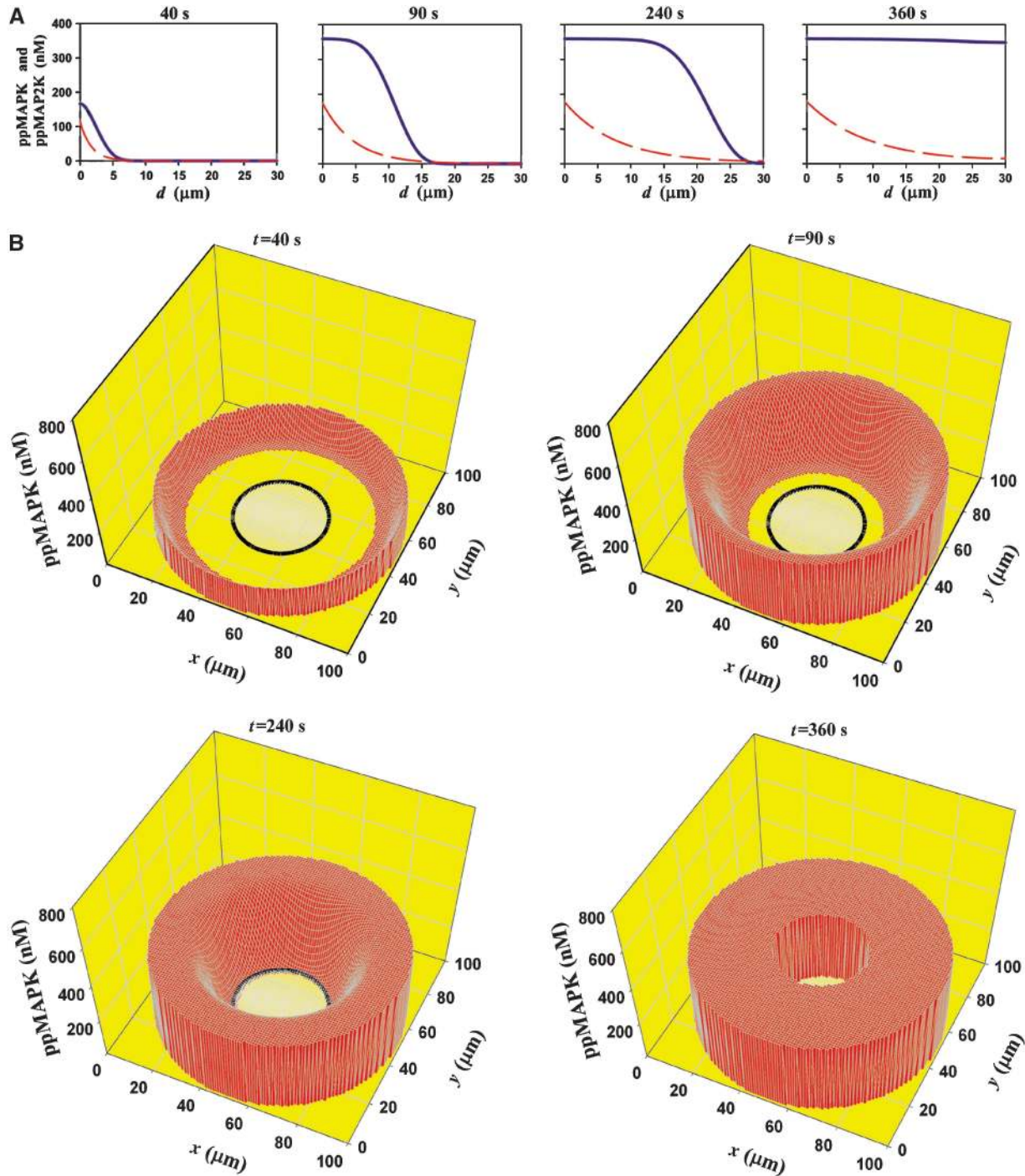


Figure 2 Phosphorylation waves emerging from the feedback inhibition of MAP2K phosphatases and bistability in the MAPK cycle. **(A)** Radial propagation profiles of the ppMAPK wave from the cell membrane (solid blue lines). Profiles of ppMAP2K are shown by dashed red lines. **(B)** Concentration profile of the ppMAPK wave for a two-dimensional cross-section taken through the center of a cell. Cell radius $L=50 \mu\text{m}$, nuclear radius $Q=20 \mu\text{m}$. The rate equations are given in Tables II and III and Supplementary Table I.

mediated endocytosis, followed by the retrograde transport of signaling endosomes containing the NGF-pTrkA complexes to the cell body (Ginty and Segal, 2002). However, data indicate that although the endosomes may carry survival signals, there must be additional mechanisms independent of the NGF transport, as tyrosine phosphorylation is observed in cell

bodies at least 30 min before the first detection of radioiodinated NGF arriving from the locally stimulated distal axons (Senger and Campenot, 1997). Lateral propagation of TrkA phosphorylation along the axon membrane is excluded, as nearly complete suppression of TrkA signaling in the cell bodies/proximal axons did not affect neuronal survival,

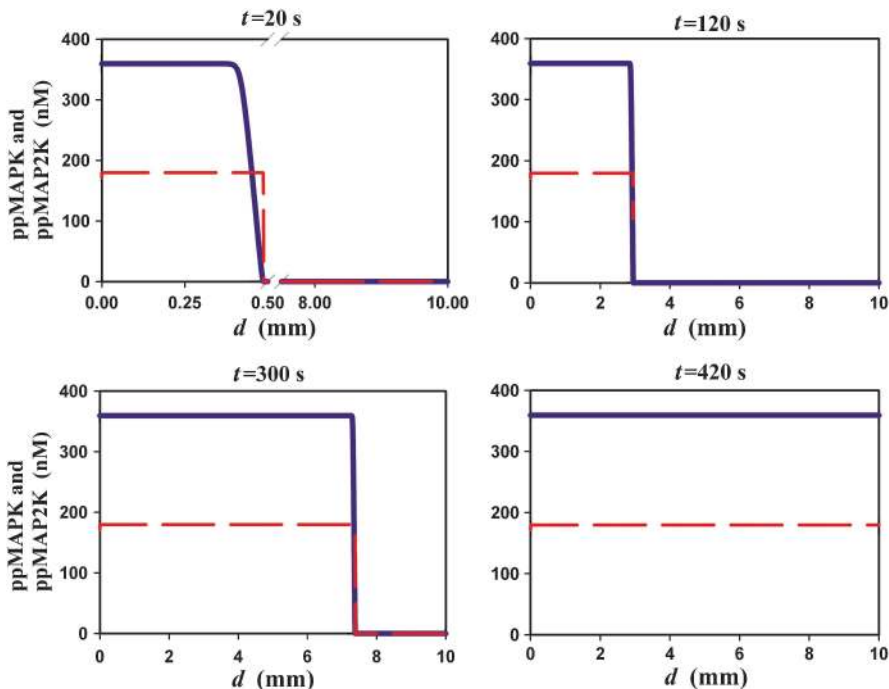


Figure 3 Traveling wave of active MAPK carrying a binary phosphorylation signal over exceedingly long distances. The ppMAPK wave propagation (one-dimensional geometry) is supported by the feedback activation of MAP2K. This wave maintains the signal magnitude and velocity and propagates over 1 cm with a velocity of 25 $\mu\text{m/s}$. Profiles of ppMAPK and ppMAP2K are shown by solid (blue) line and dashed (red) lines, respectively. The wave fronts at 20 s are shown at a higher scale resolution. See the rate equations in Tables I–III and Supplementary Table III.

whereas TrkA inhibition at distal axons induced apoptosis (MacInnis *et al*, 2003).

Our analysis suggests a novel mechanism where signals traveling along the axon are not accompanied by NGF and do not require activated TrkA in the cell body. These fast survival signals can be transmitted by a wave of protein phosphorylation in a kinase cascade, such as MAPK or PI3K/Akt cascades. If a downstream kinase stimulates the phosphorylation of an upstream kinase in the cytoplasm (directly or via a regulatory circuit), a resulting bistable switch generates a traveling cytoplasmic wave that propagates over increasingly long distances with constant amplitude and velocity (Figure 3). After reaching the target, such as the nucleus, this wave gradually turns off owing to prompt dephosphorylation of kinases in the nucleus. Thus, protein kinase/phosphatase cascades possessing positive feedback circuits in the cytoplasm can generate biological switches in space and time that are capable of propagating phosphorylation signals over exceedingly long distances.

It was proposed that bistability would make protein phosphorylation cascades capable of ‘all-or-none’ switching and allow cells to ‘remember’ a transient differentiation stimulus long after the stimulus was removed (Xiong and Ferrell, 2003). Here, we show yet another role of bistable protein kinase cascades: to support waves of phosphoproteins that propagate signals to remote cellular locations. In contrast with traveling waves previously described (Zhabotinsky and Zaikin, 1973; Slepchenko and Terasaki, 2003), phosphoprotein waves arising from bistability in MAPK cycle feature a spatially inhomogeneous activation threshold, because the ppMAP2K concentration decreases as the distance from the membrane

increases (inset to Figure 1D). Interestingly, the fact that signals spread from the cell periphery to the interior where the surface of the wave front decreases facilitates the signal propagation. Supplementary Figures S8 and S9 illustrate this space-condensing effect; at the same values of kinetic parameters, a one-dimensional wave vanishes at distances where the wave that travels inside the cell still delivers the signal.

The analysis above suggests experiments that can test whether the rapid propagation of phosphorylation signals arises from bistability in kinase cascades. Although counter-intuitive at first glance, a marked decrease in the activity of ERK phosphatases (and/or in the ERK abundance) leads to a bifurcation where the bistable ERK response becomes merely ultrasensitive (Markevich *et al*, 2004), and the input–output relationship in Figure 1C changes to the one shown in Figure 1A. Thus, the propagation of a phosphorylation wave that delivers the survival or proliferation signal may be abolished by inhibition of the phosphatase of the kinase in the bistable cascade cycle.

Signaling via phosphoprotein waves has key advantages over solely diffusive signal propagation. Owing to phosphatase activity, the phosphorylation state of a protein that diffuses in the cytoplasm will decrease much strongly than the amplitude of a phosphoprotein wave that essentially propagates a binary signal. Positive feedback emerging from cytoplasmic interactions enables protein kinase/phosphatase cascades to transmit phosphorylation signals over much longer distances than 100 μm . The velocity of the wave significantly increases with the strength of this feedback, readily reaching hundreds of $\mu\text{m/s}$ (Supplementary Figure S10). The finding that phosphorylation

Table II Kinetic description of the MAPK cascade reactions that occur at the PM

N	Reaction	Rate	Kinetic constant
1	MAP3K → pMAP3K	$v_1^m = \frac{k_1^{\text{cat}}[\text{Ras} - \text{GTP}][\text{MAP3K}]/K_{m1}}{(1 + [\text{MAP3K}]/K_{m1})} \frac{(1 + F_a([\text{ppMAPK}]/K_a)^2)}{(1 + ([\text{ppMAPK}]/K_a)^2)}$	$k_1^{\text{cat}}=0.2$ $K_{m1}=50$ $K_a=100$
2	pMAP3K → MAP3K	$v_2^m = \frac{V_{\text{max}2}[\text{pMAP3K}]/K_{m2}}{(1 + [\text{pMAP3K}]/K_{m2})}$	$V_{\text{max}2}=5$ $K_{m2}=50$
3	MAP2K → pMAP2K	$v_3^m = \frac{k_3^{\text{cat}}[\text{pMAP3K}][\text{MAP2K}]/K_{m3}}{(1 + [\text{MAP2K}]/K_{m3} + [\text{pMAP2K}]/K_{m4})}$	$k_3^{\text{cat}}=1$ $K_{m3}=130$
4	pMAP2K → ppMAP2K	$v_4^m = \frac{k_4^{\text{cat}}[\text{pMAP3K}][\text{pMAP2K}]/K_{m4}}{(1 + [\text{MAP2K}]/K_{m3} + [\text{pMAP2K}]/K_{m4})}$	$k_4^{\text{cat}}=5$ $K_{m4}=50$
5	ppMAP2K → pMAP2K	$v_5^m = \frac{V_{\text{max}5}^m[\text{ppMAP2K}]/K_{m5}^m}{(1 + [\text{ppMAP2K}]/K_{m5}^m + [\text{pMAP2K}]/K_{m6}^m + [\text{MAP2K}]/K_{i1}^m)}$	$V_{\text{max}5}^m=100$ $K_{m5}^m=100$
6	pMAP2K → MAP2K	$v_6^m = \frac{V_{\text{max}6}^m[\text{pMAP2K}]/K_{m6}^m}{(1 + [\text{ppMAP2K}]/K_{m5}^m + [\text{pMAP2K}]/K_{m6}^m + [\text{MAP2K}]/K_{i1}^m)}$	$V_{\text{max}6}^m=100$ $K_{m6}^m=100$ $K_{i1}^m=80$

Maximal rates, Michaelis and catalytic constants are expressed in nM/s, nM and s⁻¹, respectively. The concentrations of membrane-associated proteins, the corresponding K_{mi} and $V_{\text{max}i}$ ($i=1, \dots, 6$) at the membrane are related to the cytoplasmic water volume (i.e., the surface densities are multiplied by $S_{\text{pm}}/V_{\text{cell}}$, where S_{pm} is the surface area of the PM and V_{cell} is the cell volume). Total protein concentrations, which are assumed constant on the time scale considered, are as follows: $[\text{MAP3K}]_{\text{tot}}=200$, $[\text{MAP2K}]_{\text{tot}}=200$ (nM). The parameter $F_a=5$ corresponds to long positive feedback from ppMAPK (Figure 2B of the main text); if this feedback is absent, $F_a=1$ (Figure 2A and C).

Table III Kinetic description of the MAPK cascade reactions in the cytoplasm

N	Reaction	Rate	Kinetic constant
5	ppMAP2K → pMAP2K	$v_5^c = \frac{V_{\text{max}5}^c[\text{ppMAP2K}]/K_{m5}^c}{(1 + [\text{ppMAP2K}]/K_{m5}^c + [\text{pMAP2K}]/K_{m6}^c + [\text{MAP2K}]/K_{i1}^c)}$	$V_{\text{max}5}^c=250$ $K_{m5}^c=100$
6	pMAP2K → MAP2K	$v_6^c = \frac{V_{\text{max}6}^c[\text{pMAP2K}]/K_{m6}^c}{(1 + [\text{ppMAP2K}]/K_{m5}^c + [\text{pMAP2K}]/K_{m6}^c + [\text{MAP2K}]/K_{i1}^c)}$	$V_{\text{max}6}^c=250$ $K_{m6}^c=100$ $K_{i1}^c=80$
7	MAPK → pMAPK	$v_7^c = \frac{k_7^{\text{cat}}[\text{ppMAP2K}][\text{MAPK}]/K_{m7}}{(1 + [\text{MAPK}]/K_{m7} + [\text{pMAPK}]/K_{m8})}$	$k_7^{\text{cat}}=1$ $K_{m7}=50$
8	pMAPK → ppMAPK	$v_8^c = \frac{k_8^{\text{cat}}[\text{ppMAP2K}][\text{pMAPK}]/K_{m8}}{(1 + [\text{MAPK}]/K_{m7} + [\text{pMAPK}]/K_{m8})}$	$k_8^{\text{cat}}=20$ $K_{m8}=50$
9	ppMAPK → pMAPK	$v_9^c = \frac{V_{\text{max}9}[\text{ppMAPK}]/K_{m9}}{(1 + [\text{ppMAPK}]/K_{m9} + [\text{pMAPK}]/K_{m10} + [\text{MAPK}]/K_{i2})}$	$V_{\text{max}9}=380^a$ $K_{m9}=10^a$
10	pMAPK → MAPK	$v_{10}^c = \frac{V_{\text{max}10}[\text{pMAPK}]/K_{m10}}{(1 + [\text{ppMAPK}]/K_{m9} + [\text{pMAPK}]/K_{m10} + [\text{MAPK}]/K_{i2})}$	$V_{\text{max}10}=50^a$ $K_{m10}=18$ $K_{i2}=100$

^aFor the bistable MAPK cycle (Figure 1C), $K_{m9}=2$ nM, $V_{\text{max}9}=40$ nM/s and $V_{\text{max}10}=360$ nM/s. Notations and units of measurements are the same as in Table II. The total MAPK concentration equals $[\text{MAPK}]_{\text{tot}}=360$ nM.

signals can propagate as traveling waves with a constant amplitude and high velocity over distances exceeding hundreds, or even thousands of millimeters, may solve a long-standing enigma of survival signaling in neuronal biology. When short positive regulatory circuits are in place, these waves provide a robust mechanism of signal transfer along the axon. Waves of protein phosphorylation may be a widespread mechanism of intracellular signal transfer.

Materials and methods

Description of the spatio-temporal dynamics by reaction–diffusion equations

At the cell membrane, the dynamics of the MAP3K and pMAP3K concentrations is described by the ordinary differential equation (see the first row in Table I); the total concentration, $[\text{MAP3K}]_{\text{tot}}$, of these forms remains constant. Whereas the concentration of MAP3K and

pMAP3K may depend only on time, the concentrations of (un)phosphorylated kinases, MAP2K and MAPK, at the subsequent levels of the cascade depend on both the spatial coordinates and time. Table I presents the differential equations describing diffusion and phosphorylation/dephosphorylation of these kinases and the boundary conditions at the cell and nuclear surfaces. The expressions for phosphorylation and dephosphorylation rates at the PM and in the cytoplasm are given in Tables II and III. Derivations of these rate expressions are based on experimental data on the kinase and phosphatase kinetics, and were published elsewhere (Kholodenko, 2000; Markevich *et al*, 2004). Although Michaelis–Menten kinetics is used for the sake of simplicity, a mechanistic, elementary step description gives similar results.

Numerical calculations of stationary rates and concentrations, the stability analysis of steady states and the bifurcation analysis were performed using Dbsolve (Goryanin *et al*, 1999). Dbsolve 5 is freely available at http://biosim.genebee.msu.su/index_en.htm. We used a forward Euler scheme to calculate solutions to reaction–diffusion equations given in Tables I–III (for details, see Numerical methods in Supplementary information).

Supplementary information

Supplementary information is available at the *Molecular Systems Biology* website (www.nature.com/msb).

Acknowledgements

We thank Dr E Shnol for valuable discussions on numerical methods. We apologize that the Report format limitations prevented us from citing many valuable references. This work was supported by the NIH grant GM59570. The authors declare that they do not have any competing commercial interests.

References

- Bhalla US, Ram PT, Iyengar R (2002) MAP kinase phosphatase as a locus of flexibility in a mitogen-activated protein kinase signaling network. *Science* **297**: 1018–1023
- Brown GC, Kholodenko BN (1999) Spatial gradients of cellular phospho-proteins. *FEBS Lett* **457**: 452–454
- Brown GC, Hoek JB, Kholodenko BN (1997) Why do protein kinase cascades have more than one level? *Trends Biochem Sci* **22**: 288
- Ferrell Jr JE (1997) How responses get more switch-like as you move down a protein kinase cascade. *Trends Biochem Sci* **22**: 288–289
- Ginty DD, Segal RA (2002) Retrograde neurotrophin signaling: Trk-ing along the axon. *Curr Opin Neurobiol* **12**: 268–274
- Goryanin I, Hodgman TC, Selkov E (1999) Mathematical simulation and analysis of cellular metabolism and regulation. *Bioinformatics* **15**: 749–758
- Harding A, Tian T, Westbury E, Frische E, Hancock JF (2005) Subcellular localization determines MAP kinase signal output. *Curr Biol* **15**: 869–873
- Hill DB, Plaza MJ, Bonin K, Holzwarth G (2004) Fast vesicle transport in PC12 neurites: velocities and forces. *Eur Biophys J* **33**: 623–632
- Howe CL, Mobley WC (2004) Signaling endosome hypothesis: a cellular mechanism for long distance communication. *J Neurobiol* **58**: 207–216
- Kalab P, Weis K, Heald R (2002) Visualization of a Ran-GTP gradient in interphase and mitotic *Xenopus* egg extracts. *Science* **295**: 2452–2456
- Keener J, Sneyd J (1998) *Mathematical Physiology*. New York: Springer
- Khan S, Jain S, Reid GP, Trentham DR (2004) The fast tumble signal in bacterial chemotaxis. *Biophys J* **86**: 4049–4058
- Kholodenko BN (2000) Negative feedback and ultrasensitivity can bring about oscillations in the mitogen-activated protein kinase cascades. *Eur J Biochem* **267**: 1583–1588
- Kholodenko BN (2002) MAP kinase cascade signaling and endocytic trafficking: a marriage of convenience? *Trends Cell Biol* **12**: 173–177
- Kholodenko BN (2003) Four-dimensional organization of protein kinase signaling cascades: the roles of diffusion, endocytosis and molecular motors. *J Exp Biol* **206**: 2073–2082
- Kholodenko BN (2006) Cell-signalling dynamics in time and space. *Nat Rev Mol Cell Biol* **7**: 165–176
- Kim HS, Song MC, Kwak IH, Park TJ, Lim IK (2003) Constitutive induction of p-Erk1/2 accompanied by reduced activities of protein phosphatases 1 and 2A and MKP3 due to reactive oxygen species during cellular senescence. *J Biol Chem* **278**: 37497–37510
- Lipkow K, Andrews SS, Bray D (2005) Simulated diffusion of phosphorylated CheY through the cytoplasm of *Escherichia coli*. *J Bacteriol* **187**: 45–53
- MacInnis BL, Senger DL, Campenot RB (2003) Spatial requirements for TrkA kinase activity in the support of neuronal survival and axon growth in rat sympathetic neurons. *Neuropharmacology* **45**: 995–1010
- Markevich NI, Hoek JB, Kholodenko BN (2004) Signaling switches and bistability arising from multisite phosphorylation in protein kinase cascades. *J Cell Biol* **164**: 353–359
- Miaczynska M, Pelkmans L, Zerial M (2004) Not just a sink: endosomes in control of signal transduction. *Curr Opin Cell Biol* **16**: 400–406
- Murphy LO, Smith S, Chen RH, Fingar DC, Blenis J (2002) Molecular interpretation of ERK signal duration by immediate early gene products. *Nat Cell Biol* **4**: 556–564
- Niethammer P, Bastiaens P, Karsenti E (2004) Stathmin–tubulin interaction gradients in motile and mitotic cells. *Science* **303**: 1862–1866
- Perlson E, Hanz S, Ben-Yaakov K, Segal-Ruder Y, Seger R, Fainzilber M (2005) Vimentin-dependent spatial translocation of an activated MAP kinase in injured nerve. *Neuron* **45**: 715–726
- Reynolds AR, Tischer C, Verveer PJ, Rocks O, Bastiaens PI (2003) EGFR activation coupled to inhibition of tyrosine phosphatases causes lateral signal propagation. *Nat Cell Biol* **5**: 447–453
- Senger DL, Campenot RB (1997) Rapid retrograde tyrosine phosphorylation of trkA and other proteins in rat sympathetic neurons in compartmented cultures. *J Cell Biol* **138**: 411–421
- Slepchenko BM, Terasaki M (2003) Cyclin aggregation and robustness of bio-switching. *Mol Biol Cell* **14**: 4695–4706
- Wang X, Hao N, Dohllman HG, Elston TC (2006) Bistability, stochasticity, and oscillations in the mitogen-activated protein kinase cascade. *Biophys J* **90**: 1961–1978
- Xiong W, Ferrell Jr JE (2003) A positive-feedback-based bistable ‘memory module’ that governs a cell fate decision. *Nature* **426**: 460–465
- Zhabotinsky AM, Zaikin AN (1973) Autowave processes in a distributed chemical system. *J Theor Biol* **40**: 45–61